RSC Advances

PAPER

View Article Online
View Journal | View Issue



Cite this: *RSC Adv.*, 2018, **8**, 21084

# Application of hydrotalcite in soil immobilization of iodate ($IO_3^-$)†

D. Zhang, [ab] X. Y. Liu,[c] H. T. Zhao, *[a] L. Yang,[a] T. Lü[a] and M. Q. Jin[a]

Radioactive iodine is quite mobile in soil and poses threats to human health and the ecosystem. Many materials, including layered double hydroxides (LDH), have been synthesized to successfully capture iodine from aqueous environments. However, limited information is available on the application of LDH in soil to immobilize iodine species. In the present study, the feasibility of using Mg–Al–$NO_3$ LDH for retention of soil iodate ($IO_3^-$) in both batch and column systems was analyzed. The 2 : 1 Mg–Al–$NO_3$ LDH exhibited the greatest removal efficiency of $IO_3^-$ from aqueous solution, compared with 3 : 1 and 4 : 1 Mg–Al–$NO_3$ LDH. The $Mg_2$–Al–$NO_3$ LDH demonstrated a strong affinity for $IO_3^-$, with a high sorption capacity of 149 528 mg $kg^{-1}$ and a Freundlich affinity constant $K_F$ of 21 380 L $kg^{-1}$. The addition of $Mg_2$–Al–$NO_3$ LDH in soil resulted in significant retention of $IO_3^-$ in both the batch and column experiments. The affinity parameter $K_F$ of soil with the addition of 1.33% $Mg_2$–Al–$NO_3$ LDH was 136 L $kg^{-1}$, which was 28.6 times higher than soil without LDH added. Moreover, the eluted iodate percentage was only 12.9% in the soil column with the 1.33% $Mg_2$–Al–$NO_3$ LDH addition, whereas almost 43.5% iodate was washed out in the soil column without LDH addition. The results suggested that $Mg_2$–Al–$NO_3$ LDH could effectively immobilize iodate in soil without obvious interference.

Received 11th May 2018
Accepted 5th June 2018

DOI: 10.1039/c8ra04013c

rsc.li/rsc-advances



## 1. Introduction

Stable iodine ($^{127}I$) is considered an essential microelement for human health, with a recommended daily intake of between 80 and 150 mg per day.[1] However, radioactive iodine, such as $^{129}I$, $^{131}I$, is a risk-contributing contaminant of environmental and health concern due to its easy uptake and bioaccumulation through the food chain and its high radiotoxicity. A tremendous amount of radioiodine has been released into our environment not only during atomic weapon testing, spent nuclear fuel reprocessing and nuclear accidents[2,3] but also during normal operation of nuclear power plants (NPPs)[4] or discharging of medical wastewater from thyroid cancer treatments.[5] For example, in the 2011 Fukushima NPP accident, enormous amounts of radioactive iodine ($^{131}I$) were emitted into the atmosphere and ocean.[6] These long-lived radionuclides eventually move down to surface soil by wet and dry fallout or irrigation. In aqueous environments and soil systems, iodine exists mainly as iodide ($I^-$) and iodate ($IO_3^-$).[7,8] In some cases, $IO_3^-$ is the predominant iodine form, which accounts for up to approximately 70% of total iodine, with iodide and organo-iodine being minor components.[9,10] The fate and mobility of iodine in soils depend largely on its interactions with soil components. Several recent studies reported that natural organic matter (NOM), and especially its aromatic components, played an important role in the sorption of iodine to soil and/or sediment.[11–15] However, due to the lack of aromatic carbon in soil, especially soil with relatively-low organic matter, as well as its weak affinity for many geological materials, iodine species ($I^-$ and $IO_3^-$) show high mobility and, subsequently, high ecological risks.[12,16–18] Therefore, scavenging materials and remediation actions are urgently needed.

In the past decade, considerable research effort has been made toward identifying natural and synthetic materials for removing or attenuating the transport of iodine in wastewater systems or aqueous solutions.[4,19] In the literature, many materials were reported for the capture of $I^-$ and $IO_3^-$ from aqueous systems, including claystone,[20] ordinary Portland cement,[21] sulfur-terminated (001) chalcopyrite surface,[22] crystalline silver chloride,[23] metallic oxides (such as hydrous ferric oxide (HFO) and $\gamma$-$Al_2O_3$),[24] carbon-based materials (such as superfine powered activated carbon[25] and biochar[16]), magnetite nanoparticles supported on organically modified montmorillonite (MNP-OMMTs),[26] and layered double hydroxide (LDH) materials.[27,28] Several groups have investigated the potential application of LDH and related materials in the removal of iodine from aqueous solutions.[7,9,29–32] Theiss *et al.* briefly reviewed the

[a]*College of Materials and Environmental Engineering, Hangzhou Dianzi University, Hangzhou, Zhejiang 310018, China. E-mail: info-iem@hdu.edu.cn; zhangdong@hdu.edu.cn; Tel: +86-571-87713572; +86-571-86919158*

[b]*College of Environmental & Resource Sciences, Zhejiang University, Hangzhou, Zhejiang 310058, China*

[c]*Guangdong Dazhong Agribulture Science Co. Ltd, Dongguan, 523169, China*

† Electronic supplementary information (ESI) available. See DOI: 10.1039/c8ra04013c

published scientific literature, and, with further investigation, concluded that LDH is a promising iodine removal material.[33]

LDHs, minerals based on a brucite-like structure readily found in nature, contain exchangeable anions intercalated into the interlayer regions.[9] They are represented by the following general formula:

$$[M_{1-x}^{2+}M_x^{3+}(OH)_2]^{x+}[A^{n-}]_{x/n}\Delta mH_2O \quad (1)$$

where $M^{2+}$ and $M^{3+}$ are divalent (such as $Mg^{2+}$, $Fe^{2+}$ or $Ni^{2+}$) and trivalent cations (such as $Al^{3+}$, $Fe^{3+}$ or $Cr^{3+}$), respectively. $A^{n-}$ is the interlayer exchangeable anion (mainly nitrate or chloride), and the value of $x$ is equal to the molar ratio of $M^{3+}/(M^{2+} + M^{3+})$, usually $0.2 < x < 0.33$. The presence of exchangeable $A^{n-}$ and variation of identities of $M^{2+}$ and $M^{3+}$ of LDH and isostructural materials give rise to potential high selectivity and the capacity to uptake the anion of interest.[9] The LDH and related materials have been widely applied to remove various anions and oxyanions, such as iodine species ($I^-$, $IO_3^-$), fluorine ($F^-$, $BF_4^-$), chlorine ($Cl^-$, $ClO_4^-$), bromine ($Br^-$, $BrO_3^-$), chromium ($CrO_4^-$), arsenic (arsenite, arsenate), boron, anionic dye, and aniline from aqueous solutions.[33–39] The underlying mechanisms of sorption of anions by LDHs includes:[7,33] (1) anion exchange; (2) surface adsorption; and (3) reformation. Although LDH shows a relatively high potential sorption capacity for iodine anions, the presence of competing anions, including carbonate, phosphate and sulphate, has a significant impact on uptake of the target anions from an aqueous solution.[7,9,33,40] Furthermore, we must note the fact that most of the research focuses on the removal or sorption of target anions ($I^-$ or $IO_3^-$) from aqueous solutions. Only recently, a study utilizing fixed bed columns packed with LDH to removal fluoride exhibited a lower sorption capacity than the results reported for the corresponding batch methods.[41] Soil is a much complex system containing various coexisting anions without pH and Eh control, which may significantly affect the sorption efficiency of iodine by LDH. However, to date, little information is available on the application of LDH to immobilize iodine in soil system. Therefore, the retardation efficiency and mechanism of these target anions by LDH in soil systems needs further investigation.

In this study, the main objectives were to evaluate the immobilization of iodate by Mg–Al–$NO_3$ LDH in a soil system by (1) examining the sorption property of iodate on Mg–Al–$NO_3$ LDH; (2) investigating the sorption characterization of iodate in soil amended with Mg–Al–$NO_3$ LDH in a batch system; (3) evaluating the effects of Mg–Al–$NO_3$ LDH in the immobilization of iodate in soil using the column system.

# 2. Materials and methods

## 2.1 Materials

Magnesium nitrate hexahydrate ($Mg(NO_3)_2\cdot 6H_2O$), aluminium nitrate nonahydrate ($Al(NO_3)_3\cdot 9H_2O$), sodium hydroxide (NaOH), hydrochloric acid (HCl), and potassium carbonate ($K_2CO_3$) were purchased from Aladdin Reagent Co. (Shanghai). For safety, $^{127}I$ in the form of potassium iodate ($KIO_3$) was the only iodine isotope used in these experiments. All reagents were AR grade and used as received without further purification or pre-treatment.

## 2.2 Material preparation

The main sorbent used in this study was the 2 : 1 Mg/Al LDH, the preparation of which followed the description of Thiess *et al.*[27] A batch of LDH with an ideal formula of $Mg_3Al(NO_3)_7$ was prepared at pH 10 by coprecipitation method. Briefly, a NaOH solution (4.0 mol $L^{-1}$) was added dropwise into a 150 mL solution containing $Mg(NO_3)_2\cdot 6H_2O$ (0.12 mol) and $Al(NO_3)_3\cdot 9H_2O$ (0.06 mol) with vigorous magnetic stirring under a nitrogen supply. The slurry was then refluxed at 65 °C for 24 h. The residue was separated by centrifugation and washed several times with deionized, $CO_2$-free water. The product was dried at 60 °C in vacuum for 12 h, and then ground and sieved through a 0.1 mm-mesh sieve. In addition to the LDH described above, 3 : 1 and 4 : 1 Mg/Al LDH samples were also prepared by a similar coprecipitation method.

The soil sample used in this study was collected from an agricultural land near Qinshan Nuclear Power Plant. It has a pH of 7.7, 0.97% organic carbon content, and 9.00 cmol(+) $kg^{-1}$ cation exchangeable capacity (CEC), as described in our previous work.[16]

## 2.3 Characterization of the LDH samples

The X-ray diffraction (XRD) patterns of the LDH samples were collected using an X-ray diffractometer (type XD-2600), with Cu $K_\alpha$ radiation at 40 keV 35 mA. The morphologies of the LDH samples were characterized using a Sigma 500 field emission scanning electron microscope (SEM) (Zeiss, Germany). The pore size distribution and pore volume of each LDH sample were also evaluated by the Brunauer–Emmett–Teller method using a gas sorption analyzer (NOVA-1200, Quantachrome Corp., USA).

## 2.4 Batch sorption experiments and analytical method

The sorption was conducted in triplicate by a batch equilibration technique as described in our previous work.[16] Batch sorption experiments were carried out without pH control and excluding the atmosphere or dissolved carbonate, which is impractical in real world applications especially in a soil system. In the kinetic and isotherm sorption, the required portions of soil, LDHs or LDH-soil mixture (1.5 g for soil, 15 mg for LDHs, 1.5 g for LDH-soil mixture with three contents of LDH) were weighted into 22 mL centrifuge tubes containing 20 mL solutions of $IO_3^-$, with concentrations ranging from 0–200 mg $L^{-1}$. Controls without sorbents were set up in parallel to account for the possible solute loss by handling and other possible ways. After shaken for a certain kinetic time or equilibrium time (4 h based on sorption kinetics) using a temperature-controlled shaker at 150 rpm at 25 °C, the suspensions were separated by centrifuging for 20 min at 4000*g*. The supernatants were filtrated using a 0.22 μm filter membrane (ANPEL Co., Ltd, Shanghai). The concentration of iodate in the supernatants was determined following the method described in our previous work.[16] Briefly, ten millilitres of the aqueous sample was mixed

with 0.5 mL of 6.0 mol $L^{-1}$ HCl. Then, 0.5 mL of 0.1 mol $L^{-1}$ $K_2CO_3$ was added and fully mixed. After keeping the sample still for 10 min, it was measured with a spectrophotometer (Shimadzu UV-Vis 2600, Japan) at a 352 nm wavelength. The limit of detection for $IO_3^-$ was 0.6 mg $L^{-1}$.

The sorption of iodate by soil and LDH was determined using the following equation:

$$\text{Removal efficiency } (\%) = \left(1 - \frac{C_i}{C_t}\right) \times 100\% \quad (2)$$

where $C_i$ and $C_t$ (mg $L^{-1}$) represent the initial and final (at any time $t$) concentrations of iodate. The sorption capacity of the soil or LDH for iodate at time $t$, $Q_t$ (mg $kg^{-1}$), was obtained as follows:

$$Q_t = \frac{(C_i - C_t) \times V}{m} \quad (3)$$

where $V$ (mL) was the volume of the solution, which equalled 20 mL in the present study; $m$ (mg) represents the mass of sorbents and used 1500 mg of soil with and without LDH.

To determine the sorption kinetics, the obtained dynamic experimental data was fitted with the pseudo-second-order model, which can be written as follows:

$$\frac{t}{Q_t} = \frac{1}{k_2 Q_m^{\,2}} + \frac{1}{Q_m} t \quad (4)$$

where $k_2$ was the pseudo-second-order rate constant (g $mg^{-1}$ $min^{-1}$). As time approaches zero, according to the pseudo-second-order model, the initial sorption rate $h$ (mg $g^{-1}$ $min^{-1}$) was calculated as follows:

$$h = k_2 Q_e^{\,2} \quad (5)$$

The logarithmic form of the Freundlich model (original form: $Q_e = K_F C_e^{\,1/n}$) was used to calculated the Freundlich parameters and is expressed as shown in the following eqn (6):

$$\log Q_e = \log K_F + \frac{1}{n} \log C_e \quad (6)$$

where $Q_e$ is the amount adsorbed per unit weight of sorbent, mg $kg^{-1}$; $C_e$ is the equilibrium concentration, mg $L^{-1}$; $K_F$ [(mg $kg^{-1}$) (mg $L^{-1}$)$^{-1}$, equal to L $kg^{-1}$] and $n$ (dimensionless) are the Freundlich isotherm constants, describing the sorption capacity and the isotherm curvature.

### 2.5 Column experiments

The soil mixed with LDH was packed in a glass column (45 mm inner diameter, 250 mm height). The portions of LDH amended in the soil were 0, 0.66%, 1.0%, and 1.33%. Two hundred grams of the soil-LDH mixture was gently placed in the column and the height of the beds was approximately 120 mm, with a 10 mm quartz sand layer below and above the soil-LDH layer. Twenty millilitres of 200 mg $L^{-1}$ $KIO_3$ solution was added to the column from the top. Water was introduced at a constant volumetric flow rate of 2 mL $min^{-1}$ to drain off the entire $KIO_3$ solution as much as possible. Fifteen liquid samples of 10 mL were withdrawn. The collected pore water was immediately filtered by a 0.45 μm membrane filter (ANPEL Co., Ltd., China) and iodate concentrations were analysed as described above.

## 3. Results and discussion

### 3.1 Characterization of the LDH sorbents

Powder XRD patterns of three Mg–Al–$NO_3$ LDHs with different cation ratios were collected and are presented in Fig. 1. The four major peaks of all the three LDHs are located at approximately 11.5°, 22.9°, 34.6°, and 39.0°, which can be indexed to the (003), (006), (012), and (015) planes of Mg–Al hydrotalcite (JCPDS 35-0965).[37] The positions of the key peaks of all three materials (2 : 1, 3 : 1, and 4 : 1 Mg–Al–$NO_3$ LDH) showed no notable shift and no additional phases were observed, indicating that the samples prepared did indeed contain Mg–Al–$NO_3$ LDH materials. The power XRD pattern intensities of the samples shown in Fig. 1 were not scaled but an indicator of the relative crystallinity was provided. The intensities of the key peaks, including $d$003 and $d$006, increased along with the increase of the cation ratio, indicating higher crystallization with a higher cation ratio (*e.g.*, 4 : 1 Mg–Al–$NO_3$ LDH). However, all the key peaks of the three LDHs were sufficiently narrow and intense and these results verified the successful crystallization.[27]

SEM images of the three Mg–Al–$NO_3$ LDH samples showed agglomeration of platelets of irregular size and shape and were significantly affected by the cation ratio (Fig. 2). A layered structure was observed in 2 : 1 Mg–Al–$NO_3$ LDH (Fig. 2A), while the SEM image of the 4 : 1 Mg–Al–$NO_3$ LDH sample displayed microcrystalline granules embedded onto the heterogeneous matrix (Fig. 2C). The microscopy morphology results are consistent with the X-ray diffractograms and demonstrated that the relatively less crystalline heterogeneous phase in 2 : 1 Mg–Al–$NO_3$ LDH was more consistent with a hydrotalcite-like structure.[9] The average pore size distribution was approximately 10 nm (data not shown).

### 3.2 Removal of iodate ($IO_3^-$) from aqueous solution by LDH

To evaluate the ability of Mg–Al–$NO_3$ LDH to adsorb $IO_3^-$, as well as the effect of the cation (Mg/Al) ratio on the sorption of

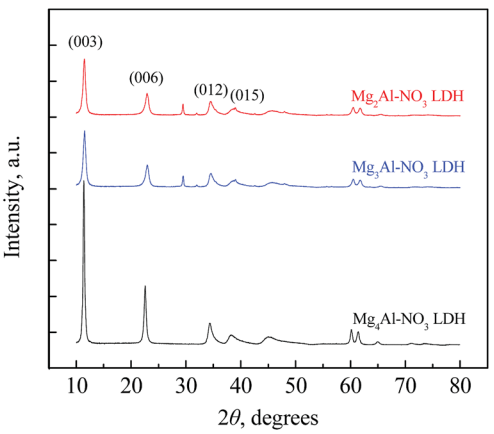


Fig. 1 XRD patterns of three MgAl–$NO_3$ LDH samples.

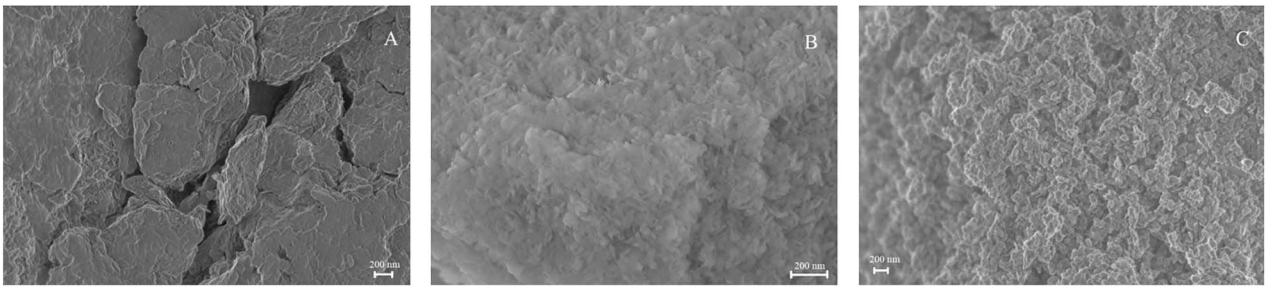


Fig. 2 SEM images of MgAl–$NO_3$ LDH samples with different Mg/Al ratios of 2 (A), 3 (B), and 4 (C).

$IO_3^-$, batch studies were performed and the results are presented in Fig. 3. The $M^{2+}$ : $M^{3+}$ cation ratio of the LDH is an important factor that influences anion uptake. The Mg/Al ratio significantly affected the iodate uptake, due to different charge density.[33] The greatest removal of $IO_3^-$ from an aqueous solution was 57.0% by 2 : 1 Mg–Al–$NO_3$ LDH, while iodate uptake of 40.5% and 28.0% were observed when using 3 : 1 and 4 : 1 Mg–Al–$NO_3$ LDH, respectively. However, the results in the present experiment appear inconsistent with those reported by Toraishi *et al.*,[42] where the 3 : 1 LDH was found to be the optimal cation ratio for iodate sorption. It is interesting to note that some studies reported that the 4 : 1 LDH was preferable for iodide sorption.[30,31] It is reasonable that the 2 : 1 LDH contains more trivalent aluminium ions and high charge density in the substituted brucite layers, which could accommodate more $IO_3^-$ compared to the 3 : 1 and 4 : 1 LDH.[27] In addition, the initial iodate concentration, LDH dosage, and temperature influenced the sorption efficiency of $IO_3^-$ from the aqueous solution (shown in Fig. S1–S3†). In the present condition (200 mg $L^{-1}$ of initial iodate concentration, 0.75 g $L^{-1}$ of LDH dosage, and 25 °C), the removal efficiency of $IO_3^-$ by $Mg^2$–Al–$NO_3$ LDH was comparable or even higher than that previously reported.[9,36]

All the three Mg–Al–$NO_3$ LDHs showed large iodate sorption capacities, as shown in Fig. 3. Similarly, the 2 : 1 Mg–Al–$NO_3$ LDH showed the largest sorption capacity of 149 528 mg $IO_3^-$ $kg^{-1}$, followed by 106 882 and 73 414.3 mg $kg^{-1}$ for the 3 : 1 and 4 : 1 Mg–Al–$NO_3$ LDH, respectively. Furthermore, Mg–Al–$NO_3$ LDH had a much greater sorption capacity for anions, compared to Ni–Al-LDH and Zn–Al-LDH.[9,34] Therefore, the 2 : 1 Mg–Al–$NO_3$ LDH was chosen to use in the majority of the following immobilization studies.

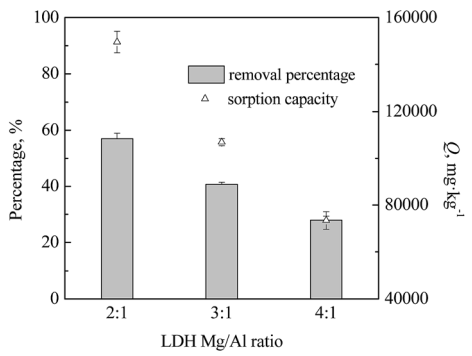


Fig. 3 Effect of the cation ratio on the sorption of $IO_3^-$ by Mg–Al–$NO_3$ LDHs.

### 3.3 Effects of $Mg_2$–Al–$NO_3$ LDH on the soil sorption of $IO_3^-$ in the batch system

Fig. 4A shows the kinetic sorption behaviour of iodate ions by soil, $Mg_2$–Al–$NO_3$ LDH, and soil amended with 1% of LDH. The iodate sorption by all three sorbents exhibited a biphasic phenomenon: a steep initial ascending trend of sorption capacity ($Q_t$), followed by a steady but slower accumulation.

The equilibriums were achieved in less than 240 minutes for soil, soil amended with LDH and pure $Mg_2$–Al–$NO_3$ LDH. The soil has a very weak affinity, with the sorption capacity of 59.2 mg $kg^{-1}$, which was consistent with previous observations

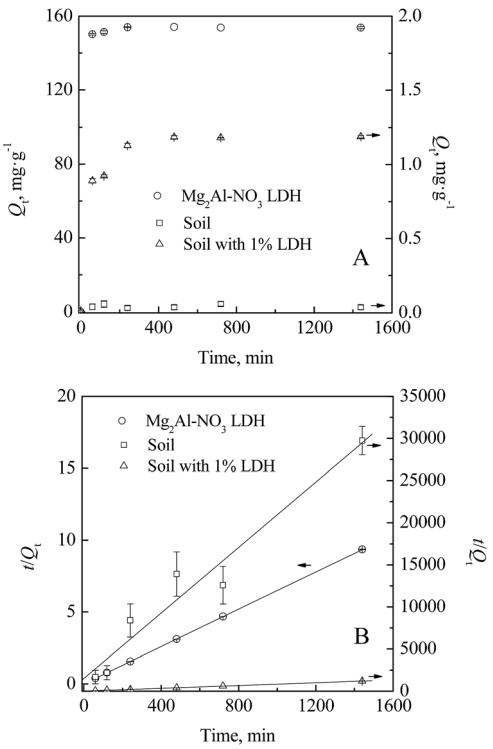


Fig. 4 Kinetic sorption of $IO_3^-$ by soil in the absence and presence of $Mg_2$Al–$NO_3$ LDH: (A) sorption capacity; (B) simulation with the pseudo-second-order model.

Table 1 Kinetic parameters of iodate onto the LDH, soil and soil-LDH mixture using the pseudo-second order model

| Sorbent | $k_2$, g mg$^{-1}$ min$^{-1}$ | $Q_m$, mg g$^{-1}$ | $h$, mg g$^{-1}$ min$^{-1}$ | $R^2$ |
|---|---|---|---|---|
| $Mg_2Al$–$NO_3$ LDH | 0.00768 | 153.8 | 182 | 0.9999 |
| Soil | 0.25307 | 0.05142 | 0.000669 | 0.9499 |
| Soil with 1% LDH | 0.03769 | 1.210 | 0.0552 | 0.9998 |

and follows the range of 25–70 mg kg$^{-1}$ reported in the literature.[16,18,43] The $Mg_2$–Al–$NO_3$ LDH showed an enormous maximum sorption capacity, up to 154.2 mg g$^{-1}$, which is more than 2600 times higher than that of the soil. Therefore, with the addition of only 1% of $Mg_2$–Al–$NO_3$ LDH to soil, the sorption capacity can reach 20 times higher (1187 mg kg$^{-1}$) than that of soil.

The pseudo-second-order model has been applied to the kinetic sorption data shown Fig. 4B. The calculated constants ($k_2$, $Q_m$, $h$) as well as the regression coefficients ($R^2$) are listed in Table 1 and demonstrate that the experimental data fit well to the pseudo-second-order model. It was surprising that the $Mg_2$–Al–$NO_3$ LDH had the lowest pseudo-second-order rate constant ($k_2$) of 0.00768 g mg$^{-1}$ min$^{-1}$, while the greatest $k_2$ was obtained in the soil system (0.25307 g mg$^{-1}$ min$^{-1}$). This is probably due to the quite small iodate sorption capacity ($Q_m$, 0.05142 g g$^{-1}$) of soil, which is easily reaches equilibrium. Instead, the initial sorption rate $h$ might be a better parameter to reveal the kinetics of iodate sorption. As seen in Table 1, it's much more reasonable that the calculated $h$ followed the order: $Mg_2$–Al–$NO_3$ LDH > soil amended with 1% LDH > soil, with $h$ values of 0.000669, 0.0552, and 182 mg g$^{-1}$ min$^{-1}$. Moreover, the values of $Q_m$ calculated from the pseudo-second-order model are very close to the measured values. The pseudo-second-order model is based on the assumption that chemisorption is the rate-limiting step, involving valence forces through the sharing or exchange of electrons between sorbent and sorbate.[41] Therefore, the observations in this study indicated that the second order adoption reaction and diffusion process may be the limiting step.[29]

Adsorption isotherms were analysed to investigate the adsorption capacity and affinity of LDH and soil with $IO_3^-$ at different equilibrium concentrations and shown in Fig. 5. Again, the $Mg_2$–Al–$NO_3$ LDH showed a larger iodate sorption amount than that of the soil (Fig. 5A). With the increase of the addition portion of LDH in the soil (0.66% to 1.33%), the sorption capacity subsequently increased. The isothermal sorption data of $IO_3^-$ onto the soil, $Mg_2$–Al–$NO_3$ LDH, and their mixtures were plotted and fitted well to the Freundlich model (Fig. 5B). The calculated Freundlich parameters are summarized in Table 2. The $Mg_2$–Al–$NO_3$ LDH demonstrated very high affinity for $IO_3^-$ ($K_F$ reaches 21 380 L kg$^{-1}$), which is much higher than the ones reported in other studies.[9] It is reasonable to note that the high removal of $IO_3^-$ from the aqueous solution was observed across the initial test concentration range (40–300 mg L$^{-1}$) (Fig. S1†). Moreover, the addition of $Mg_2$–Al–$NO_3$ LDH in the soil at a relatively low dosage also exhibited a higher sorption affinity for $IO_3^-$, compared with the soil ($K_F$ value of 4.74 L kg$^{-1}$). The $K_F$ values were 13.1, 26.4, and 136 L kg$^{-1}$ for 0.66%, 1%, and 1.33% additions of LDH, respectively.

More importantly, the ratio between the $K_F$ values of $Mg_2$–Al–$NO_3$ LDH and that of the soil ($K_F$*/$K_{F,\ soil}$), representing the

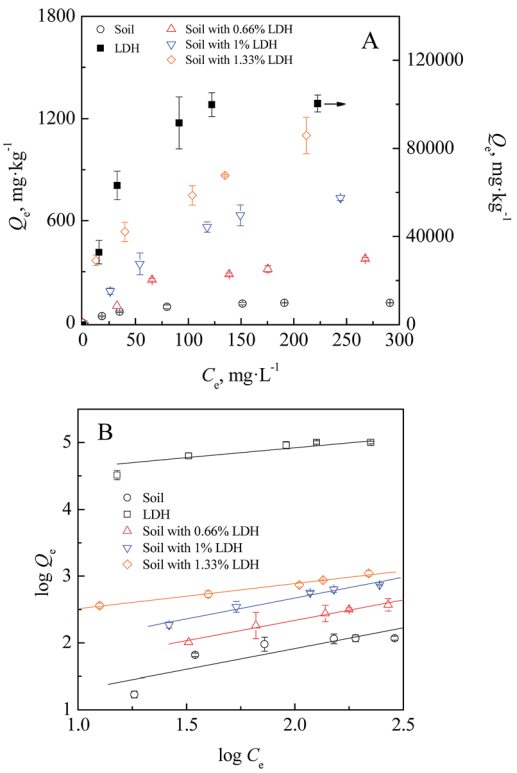


Fig. 5 Isotherm sorption of $IO_3^-$ by soil in the absence and presence of $Mg_2Al$–$NO_3$ LDH: (A) sorption capacity; (B) stimulated with the Freundlich model.

Table 2 Isothermal sorption parameters of iodate onto soil with and without LDH[a]

| | Freundlich parameters | | | |
|---|---|---|---|---|
| Sorbent | $K_F$, L kg$^{-1}$ | $n$ | $R^2$ | $K_F$*/$K_{F,\ soil}$ |
| Soil | 4.7402 | 1.61 | 0.7616 | |
| LDH | 21 380 | 3.38 | 0.8864 | 4510 |
| Soil with 0.66% LDH | 13.086 | 1.64 | 0.9845 | 2.761 |
| Soil with 1% LDH | 26.363 | 1.60 | 0.9730 | 5.562 |
| Soil with 1.33% LDH | 135.55 | 2.64 | 0.9900 | 28.60 |

[a] $K_F$*: Freundlich isothermal sorption parameter of iodate for LDH and soil mixed with LDH, $K_{F,\ soil}$: Freundlich isothermal sorption parameter of iodate for soil.

enhancement level of iodate sorption affinity of sorbent as a soil amendment, was quite large, *i.e.*, 4510 for $IO_3^-$. In our previous work, biochar was used as an effective soil amendment to immobilize iodide and iodate in arable land soil, due to the specific I–C interaction of the iodine anion ($I^-$ and $IO_3^-$) with the aromatic structure of biochar.[11,16] Many studies have reported that various LDH types had high affinity for iodine anions through anion exchange, surface adsorption, and the reconstruction effect.[4,27–29,33,36] Given the high potential immobilization ability of LDH, we applied 0.66%, 1%, and 1.33% of $Mg_2$–Al–$NO_3$ LDH to immobilize the behaviour of iodate in the soil system. The results exhibited that the addition of LDH could significantly enhance the sorption affinity of soil, with $K_F$*/$K_{F,\ soil}$ values of 2.761, 5.562, and 28.60. The retarding effects of LDH on the transport behaviour of iodate in soil were further analysed in continuous systems.

### 3.4 Effects of $Mg_2$–Al–$NO_3$ LDH on the soil immobilization of $IO_3^-$ in the continuous systems

Laboratory column flushing was conducted to evaluate the performance of $Mg_2$–Al–$NO_3$ LDH in retarding soil $IO_3^-$. The instantaneous effluent concentration of $IO_3^-$ from soil columns with different $Mg_2$–Al–$NO_3$ LDH additions are plotted in Fig. 6A *versus* the elution volume. With an increasing elution volume, a similar tendency of the effluent iodate concentration was shared by all the four soil-LDH mixture systems. That is, a sharp increase of iodate concentration to maximum value in the outlet is observed, followed a gradual decrease to a relatively low level. However, the addition of the $Mg_2$–Al–$NO_3$ LDH postponed the appearance of the effluent peak and sharply decreased the maximum concentration. Additionally, it can be seen that the changes had an apparent dependence on the portion of $Mg_2$–Al–$NO_3$ LDH. For example, the maximum value of effluent iodate (59 mg $L^{-1}$) appeared at the volume of 20 mL in soil, while in soil amended with 1.33% of $Mg_2$–Al–$NO_3$ LDH, it reached a maximum value of 6.08 mg $L^{-1}$ at the volume of 110 mL. The results can be explained by the mass transfer phenomena that takes place in the column flushing. The added $Mg_2$–Al–$NO_3$ LDH improved the affinity of soil with $IO_3^-$ as mentioned above, which reduced the desorption of $IO_3^-$ from the solid matrix. The eluted amount of $IO_3^-$ *versus* the total amount of $IO_3^-$ ($m/m_0$) were also calculated and are shown in Fig. 6B. Similarly, the $m/m_0$ values in all systems increased sharply and gradually decreased to a relatively small level.

Moreover, the total eluted percentage (%) of $IO_3^-$ was calculated using the total eluted amount of $IO_3^-$ *versus* the total amount of $IO_3^-$ ($\Sigma m/m_0$), which is illustrated in Fig. 6C. The application of $Mg_2$–Al–$NO_3$ LDH significantly retarded the mobility of iodate in soil. The eluted percentage of $IO_3^-$ reduced with the increase of added $Mg_2$–Al–$NO_3$ LDH, from 43.5% in soil to 21.0%, 16.4%, and 12.9% for 0.66%, 1%, and 1.33% LDH additions, respectively. Additionally, the increase in elution volume (or time) of treated solution to reach a stable maximum was also observed when the LDH addition increased. For instance, it only needs a 60 mL solution to wash out more than 40% of the $IO_3^-$ in the soil system; however, more than 110 mL

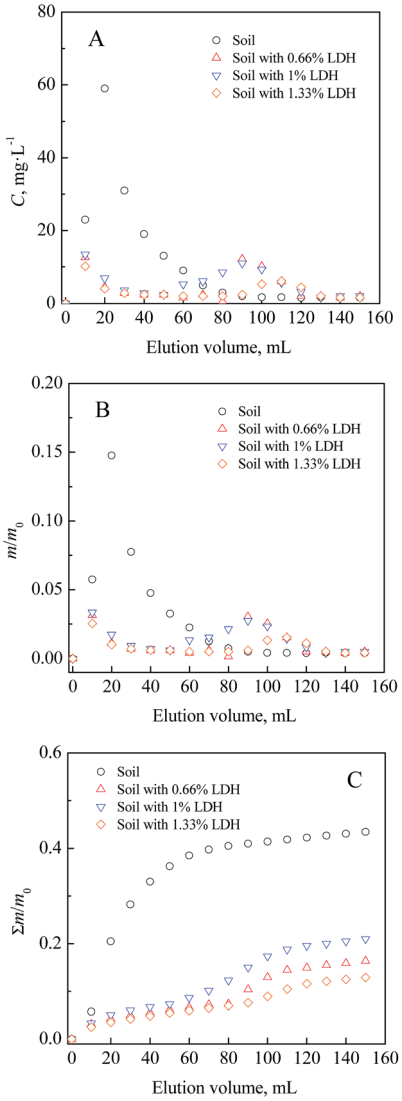


Fig. 6 Effects of the $Mg_2Al$–$NO_3$ LDH addition on the $IO_3^-$ concentration: (A) instantaneous effluent concentration; (B) accumulated $IO_3^-$ amount; (C) total amount of eluted $IO_3^-$.

of solution is needed to achieve the flushing plateau with the addition of 1% $Mg_2$–Al–$NO_3$ LDH. Soil was considered a weak matrix to maintain iodine species such as iodide and iodate.[12,16–18] In the literature, many materials have been synthetized to capture these mobile compounds from aqueous solutions.[16,22–28] However, the efficiencies of these excellent materials should be further examined in soil due to the interferences of variables in real world applications.[27] For example, affinity parameters were obtained ranged from 363 to 2240 L $kg^{-1}$ by Co–Cr and Ni–Cr hydrotalcite,[9] and 600 to 900 L $kg^{-1}$ by microporous acetyl cellulose membrane.[4] The efficiency in the column study was comparable to that obtained in the batch experiments, without obvious adverse effects by the soil variables, such as coexisting ions and soil pH. The results indicated that $Mg_2$–Al–$NO_3$ LDH could potentially be applied to effectively immobilize iodate in soil.

## 4. Conclusions

The $Mg_2$–Al–$NO_3$ LDH has been successfully synthesized and applied to immobilize iodate in soil in both the batch and column systems. The $Mg_2$–Al–$NO_3$ LDH demonstrated a strong affinity for $IO_3^-$, with a high removal efficiency of 57.0% and a sorption capacity of 149 528 mg $kg^{-1}$. The cation ratio (Mg : Al in this study) was an important factor influencing the iodate sorption capacity. The capacities were 106 882 and 73 414.3 mg $kg^{-1}$ for the 3 : 1 and 4 : 1 Mg–Al–$NO_3$ LDH samples, respectively, which was much lower than that of the 2 : 1 LDH. The addition of $Mg_2$–Al–$NO_3$ LDH in soil with different portions resulted in significant retention of $IO_3^-$ in both the batch and column experiments. For example, the affinity parameter $K_F$ of soil with 1.33% $Mg_2$–Al–$NO_3$ LDH added was 136 L $kg^{-1}$, which was 28.6 times higher than soil without an LDH addition. Moreover, the eluted iodate percentage was only 12.9% in the soil column with the 1.33% $Mg_2$–Al–$NO_3$ LDH addition, whereas almost 43.5% iodate was washed out in the soil column without LDH addition. The results suggested that LDH could effectively immobilize iodate in soil without obvious interference by coexist ions.

## Conflicts of interest

There are no conflicts to declare.

## Acknowledgements

This work was supported by the National Natural Science Foundation of China (21407037 and 41271249), Project of the Natural Science Foundation of Zhejiang Province (LQ14B070006), and the Special Funding for Introduced Innovative R&D Team of Dongguan (2014607101003).

## References

1 *Guidelines for drinking-water quality*, WHO press, World Health Organization, Geneva, Switzerland, 2011.
2 S. Xu, S. Freeman, X. Hou, A. Watanabe, K. Yamaguchi and L. Zhang, Iodine isotopes in precipitation: temporal responses to $^{129}I$ emissions from the Fukushima nuclear accident, *Environ. Sci. Technol.*, 2013, **47**, 10851–10859.
3 X. Hou, A. Aldahan, S. Nielsen and G. Possnert, Time series of $^{129}I$ and $^{127}I$ speciation in precipitation from Denmark, *Environ. Sci. Technol.*, 2009, **43**, 6522–6528.
4 S. Kulyukhin, Fundamental and applied aspects of the chemistry of radioactive iodine in gas and aqueous media, *Russ. Chem. Rev.*, 2012, **81**, 960.
5 P. Rose, R. Swanson and J. Cochran, Medically-derived $^{131}I$ in municipal sewage effluent, *Water Res.*, 2012, **46**, 5663–5671.
6 K. Hirose, 2011 Fukushima Dai-ichi nuclear power plant accident: summary of regional radioactive deposition monitoring results, *J. Environ. Radioact.*, 2012, **111**, 13–17.
7 L. Iglesias, C. Walther, F. Medina, A. Hölzer, A. Neumann, M. Lozano-Rodriguez, M. Álvarez and N. Torpapava, A comprehensive study on iodine uptake by selected LDH phases *via* coprecipitation, anionic exchange and reconstruction, *J. Radioanal. Nucl. Chem.*, 2016, **307**, 111–121.
8 X. Hou, V. Hansen, A. Aldahan, G. Possnert, O. Lind and G. Lujaniene, A review on speciation of iodine-129 in the environmental and biological samples, *Anal. Chim. Acta*, 2009, **632**, 181–196.
9 T. Levitskaia, S. Chatterjee, B. Arey, E. Campbell, Y. Hong, L. Kovarik, J. Peterson, N. Pence, J. Romero, V. Shutthanandan, B. Schwenzer and T. Varga, RedOx-controlled sorption of iodine anions by hydrotalcite composites, *RSC Adv.*, 2016, **6**, 76042–76055.
10 D. Kaplan, M. Denham, S. Zhang, C. Yeager, C. Xu, K. Schwehr, H. Li, F. Ho, D. Wellman and P. Santschi, Radioiodine biogeochemistry and prevalence in groundwater, *Crit. Rev. Environ. Sci. Technol.*, 2014, **44**, 2287–2335.
11 S. Choung, W. Um, M. Kim and M. Kim, Uptake mechanism for iodine species to black carbon, *Environ. Sci. Technol.*, 2013, **47**, 10349–10355.
12 C. Xu, E. Miller, S. Zhang, H. Li, Y. Ho, K. Schwehr, D. Kaplan, S. Otosaka, K. Roberts, R. Brinkmeyer, C. Yeager and P. Santschi, Sequestration and remobilization of radioiodine ($^{129}I$) by soil organic matter and possible consequences of the remedial action at Savannah River Site, *Environ. Sci. Technol.*, 2011, **45**, 9975–9983.
13 C. Xu, S. Zhang, Y. Sugiyama, N. Ohte, Y. Ho, N. Fujitake, D. Kaplan, C. Yeager, K. Schwehr and P. Santschi, Role of natural organic matter on iodine and $^{239,240}Pu$ distribution and mobility in environmental samples from the northwestern Fukushima Prefecture, Japan, *J. Environ. Radioact.*, 2016, **153**, 156–166.
14 P. Santschi, C. Xu, S. Zhang, K. Schwehr, R. Grandbois, D. Kaplan and C. Yeager, Iodine and plutonium association with natural organic matter: a review of recent advances, *Appl. Geochem.*, 2017, **85**, 121–127.
15 Y. Unno, H. Tsukada, A. Takeda, Y. Takaku and S. Hisamatsu, Soil–soil solution distribution coefficient of soil organic matter is a key factor for that of radioiodide in surface and subsurface soils, *J. Environ. Radioact.*, 2017, **169–170**, 131–136.
16 D. Zhang, L. Lu, T. Lü, M. Jin, J. Lin, X. Liu and H. Zhao, Application of a rice husk-derived biochar in soil immobilization of iodide ($I^-$) and iodate ($IO_3^-$), *J. Environ. Radioact.*, 2018, **18**, 1540–1547.
17 G. Lefèvre, J. Bessière, J. Ehrhardt and A. Walcarius, Immobilization of iodide on copper(I) sulfide minerals, *J. Environ. Radioact.*, 2003, **70**, 73–83.
18 W. Shetaya, S. Young, M. Watts, E. Ander and E. Bailey, Iodine dynamics in soils, *Geochim. Cosmochim. Acta*, 2012, **77**, 457–473.
19 B. Riley, J. Vienna, D. Strachan, J. McCloy and J. Jerden, Materials and processes for the effective capture and immobilization of radioiodine: a review, *J. Nucl. Mater.*, 2016, **470**, 307–326.

 

20 S. Savoye, B. Frasca, B. Grenut and A. Fayette, How mobile is iodide in the Callovo–Oxfordian claystones under experimental conditions close to the *in situ* ones?, *J. Contam. Hydrol.*, 2012, **142–143**, 82–92.

21 M. Atkins and F. Glasser, Application of Portland cement-based materials to radioactive waste immobilization, *Waste Management*, 1992, **12**, 105–131.

22 K. Li, Y. Zhao, P. Zhang, C. He, J. Deng, S. Ding and W. Shi, Combined DFT and XPS investigation of iodine anions adsorption on the sulfur termination (001) chalcopyrite surface, *Appl. Surf. Sci.*, 2016, **390**, 412–421.

23 M. Mostafa, H. Ramadan and M. El-Amir, Sorption and desorption studies of radioiodine onto silver chloride *via* batch equilibration with its aqueous media, *J. Environ. Radioact.*, 2015, **150**, 9–19.

24 T. Nagata and K. Fukushi, Prediction of iodate adsorption and surface speciation on oxides by surface complexation modeling, *Geochim. Cosmochim. Acta*, 2010, **74**, 6000–6013.

25 M. Ikari, Y. Matsui, Y. Suzuki, T. Matsushita and N. Shirasaki, Removal of iodide from water by chlorination and subsequent adsorption on powered activated carbon, *Water Res.*, 2015, **68**, 227–237.

26 J. Jiang and D. Lee, Magnetite nanoparticles supported on organically modified montmorillonite for adsorptive removal of iodide from aqueous solution: optimization using response surface methodology, *Sci. Total Environ.*, 2018, **615**, 549–557.

27 F. Theiss, G. Ayoko and R. Frost, iodide removal using LDH technology, *Chem. Eng. J.*, 2016, **296**, 300–309.

28 F. Theiss, G. Ayoko and R. Frost, Leaching of iodide ($I^-$) and iodate ($IO_3^-$) anions from synthetic layered double hydroxide materials, *J. Colloid Interface Sci.*, 2016, **478**, 311–315.

29 F. Theiss, G. Ayoko and R. Frost, Sorption of iodide ($I^-$) from aqueous solution using Mg/Al layered double hydroxides, *Mater. Sci. Eng., C*, 2017, **77**, 1228–1234.

30 G. Fetter, E. Ramos, M. Olguin, P. Bosch, T. López and S. Bulbulian, Sorption of $^{131}I^-$ by hydrotalcites, *J. Radioanal. Nucl. Chem.*, 1997, **221**, 63–66.

31 L. Linag and L. Li, Adsorption behavior of calcined layered double hydroxides towards removal of iodide contaminants, *J. Radioanal. Nucl. Chem.*, 2006, **273**, 221–226.

32 T. Toraishi, S. Nagasaki and S. Tanaka, Adsorption behavior of $IO_3^-$ by $CO_3^{2-}$ and $NO_3^-$-hydrotalcite, *Appl. Clay Sci.*, 2002, **22**, 17–23.

33 F. Theiss, S. Couperthwaite, G. Ayoko and R. Frost, A review of the removal of anions and oxyanions of the halogen elements from aqueous solution by layered double hydroxides, *J. Colloid Interface Sci.*, 2014, **417**, 356–368.

34 L. Lv, J. He, M. Wei, D. Evans and X. Duan, Factors influencing the removal of fluoride from aqueous solution by calcined Mg–Al–$CO_3$ layered double hydroxides, *J. Hazard. Mater.*, 2006, **133**, 119–128.

35 A. Ay, B. Zümreoglu-Karan and A. Temel, Boron removal by hydrotalcite-like, carbonate-free Mg–Al–$NO_3$-LDH and a rationale on the mechanism, *Microporous Mesoporous Mater.*, 2007, **98**, 1–5.

36 S. Yu, X. Wang, Z. Chen, J. Wang, S. Wang, T. Hayat and X. Wang, Layered double hydroxide intercalated with aromatic acid anions for the efficient capture of aniline from aqueous solution, *J. Hazard. Mater.*, 2017, **321**, 111–120.

37 C. Lei, X. Zhu, B. Zhu, C. Jiang, Y. Le and J. Yu, Superb adsorption capacity of hierarchical calcined Ni/Mg/Al layered double hydroxides for Congo red and Cr(VI) ions, *J. Hazard. Mater.*, 2017, **321**, 801–811.

38 D. Tang and G. Zhang, Efficient removal of fluoride by hierarchical Ce–Fe bimetal oxides adsorbent: thermodynamics, kinetics and mechanism, *Chem. Eng. J.*, 2016, **283**, 721–729.

39 L. Yang, Z. Shahrivari, P. Liu, M. Sahimi and T. Tsotsis, Removal of trace levels of arsenic and selenium from aqueous solutions by calcined and uncalcined layered double hydroxides (LDH), *Ind. Eng. Chem. Res.*, 2005, **44**, 6804–6815.

40 B. Hunter, W. Hieringer, J. Winkler, H. Gray and A. Müller, Effect of interlayer anions on [NiFe]-LDH nanosheet water oxidation activity, *Energy Environ. Sci.*, 2016, **9**, 1734.

41 M. Jiménez-Núñez, M. Solache-Ríos and M. Olguín, Fluoride sorption from aqueous solutions and drinking water by magnesium, cobalt, and nickel hydrotalcite-like compounds in batch and column systems, *Sep. Sci. Technol.*, 2010, **45**, 786–793.

42 T. Toraishi, S. Nagasaki and S. Tanaka, Adsorption behavior of $IO_3^-$ by $CO_3^{2-}$ and $NO_3^-$- hydrotalcite, *Appl. Clay Sci.*, 2002, **22**, 17–23.

43 C. Hong, H. Weng, G. Jilani, A. Yan, H. Liu and Z. Xue, Evaluation of iodide and iodate for adsorption–desorption characteristics and bioavailability in three types of soil, *Biol. Trace Elem. Res.*, 2012, **146**, 262–271.